# Thermal Analysis and Creep Curve for Some Sn-Ag-Cu Compositions

M.Sc. Abdullah Tayser Abdullah Mulla`a

## Abstract:

In this work have been investigated the mechanical properties, thermal analysis of Sn–3.5Ag, Sn-3.5Ag-0.5Cu, Sn-3.5Ag-1.0Cu, Sn-3.5Ag-1.5Cu and Sn-3.5Ag-2.0Cu ternary alloys. The samples were prepared from Tin, Sliver and Copper with high purity of 99.99%. The melting point was determined by (DSC). The results showed that with the addition of small amount of Cu elements, the melting point was changed for all alloys.

Results showed that (SAC) solders, which containing a small amount of Cu element, exhibited significantly improved creep resistance and the creep time to failure also increased. The improvement in creep resistance can be attributed to the presence of Cu, which aid to resist the motion of the dislocations and there is observed the activation energies were stress dependent for each solder system 9.8 MPa, 11.76 MPa. Also that The sensitivity rate, increases with increasing temperature.

*Keywords:*Lead-free solder / Sn–Ag–Cu alloy / Thermal Properties / Creep Curve / Sensitivity Rate / Activation Energy

## الملخص بالعربي:

تقوم هذه على دراسة الخواص الميكانيكية، الحرارية للسبائك الثلاثية *Sn-3.5Ag*، *Sn-3.5Ag-0.5Cu*، *Sn-3.5Ag-1.0Cu*، *Sn-3.5Ag-1.5Cu* *Sn-3.5Ag-2.0Cu*، وقد تم التحقيق منها. وتحضير العينات من عناصر القصدير، الفضة والنحاس بنقاوة عالية (99.99%). أظهرت النتائج أن نقطة الانصهار لعينة سهله الانصهار تتأثر بإضافة النحاس لها بشكل واضح لجميع السبائك .

نتائج منحنيات الزحف تظهر بأن السبائك التي تحتوي على كمية صغيره من النحاس تظهر تحسناً في مقاومة الزحف ووقت الفشل. ويمكن أن يعزى سبب التحسن في مقاومة الزحف إلى مقاومة حركة التشوه بسبب وجود النحاس. طاقة التنشيط تبين أقل طاقه تستهلك ضرورية لصهر سبائك اللحام أيضاً معيار الحساسية يزداد مع زيادة درجة حرارة التشوه لسبيكة.

كلمات دالة: اللحامات الخالية من الرصاص / سبائك Sn–Ag–Cu / الخواص الحرارية / منحنى الزحف / معدل الحساسية / طاقة التنشيط.

## Introduction:

The microelectronics industry continues to include expanding and evolving topics and technologies as the demands for smaller, faster and lighter products. To achieve higher circuit board component densities, package dimensions have been shrinking. Although the electronics industry has made considerable advances over the past few decades, the essential requirements of communications among all types of components in all electronic systems remain unchanged. Components need to be electrically connected for power, ground and signal transmissions. Solders play an important role in any electronic assembly. They are used in different levels of the electronics assembly and act, in the same time, as heat dissipaters and stress relievers [1-3].

However, due to concerns about the toxicity of *Pb*, restrictions have been implemented on the use of *Pb* in solder alloys. In fact, the European Union (EU) has enacted legislation known as the Restrictions Of Hazardous Substances (ROHS), that limits the maximum *Pb* content in the solder alloys to 0.1% by weight as of July 2006 on all electronic products entering the EU market. Lead is a naturally-occurring element that can be harmful to humans when ingested or inhaled particularly to children under the age of six years. Lead particles in the environment can attach to dust and be carried long distances in the air. Such lead-containing dust can be removed from the air by rain and deposited on surface soil where it may remain for many years. In addition, heavy rains may cause lead in surface soil to migrate into ground water and eventually into water systems [3-4].

For more than 50 years, solders containing lead have been used almost exclusively throughout the electronics industry for attaching components to Printed Wiring Boards (PWBs). The *Sn-Pb* solder is the most widely utilized

soldering alloy, the popularity of this alloy is due to its relatively low melting temperature, aggressive bonding characteristics, good electrical continuity and low cost.

Nontoxic substitute materials should satisfy a number of criteria if they are to serve as an effective replacement for lead. Tin is the basic material for the introduction of lead-free alloys. The reasons for the use of tin are due to its low costs, world-wide availability, excellent physical, good electrical and thermal properties. Tin is the basis of the group of the *Sn-Pb* solders currently used. There have been numerous new lead-free solders invented over the past ten years as replacement alloys. The characteristics of these alloys which should be tested and monitored are:

Good

| | |
|---|---|
| • Melting temperature close to tin/lead solders (185 °C)<br>• Relatively non-toxic<br>• Availability<br>• Low cost | • Good wetting properties<br>• Adequate thermal conductivity and shelf life stability<br>• Good mechanical strength (creep strength-ultimate tensile strength)<br>• Good resistance of fatigue |

electrical and thermal conductivity properties are also necessary since the solder alloy is commonly used as an electrical contact as well as being the principle source of attachment for the microelectronic devices. An example of this is seen in the popular controlled collapse chip connections where the solder alloy acts as the electrical connection, a thermal via and the attachment for the device itself. The shelf life stability, mechanical strength and good fatigue resistance are obvious characteristics that are crucial for producing a quality and durable product. High on the list of requisite mechanical properties are good strength, ductility and fatigue resistance. Because conductivity and joint strength depend on the significant extent of the area which contact between solder and component, the solder must sufficiently wet the components to which it bonds. The lead-free solder must incorporate all of these characteristics if it is used as a replacement since the leaded solders have already set the standards for strength and longevity [5-6].

## Experimental Procedures:

This part represents the experimental procedure and instruments that used to obtain the results of the present investigations. The initial step begins with the preparation of five solder alloys, followed by systematic measurements to recognize the mechanical, thermal and microstructural properties of the selected solder alloys. The melting point of solders were analyzed using a Differential Scanning Calorimetry (DSC). Moreover, the practical methods and instruments that used for tensile tests are explained.

Some lead-free eutectic alloys, *Sn-Ag-Cu* (SAC family), have been studied in this work. The composition and the melting points of the selected solder alloys (A) *Sn-3.5 wt% Ag*, (B) *Sn-3.5 wt% Ag-0.5 wt% Cu*, (C) *Sn-3.5 wt% Ag-1.0 wt% Cu*, (D) *Sn-3.5 wt% Ag-1.5 wt% Cu* and (E) *Sn-3.5 wt% Ag-2.0 wt% Cu* are shown in Table (3 - 1).These compositions were prepared using pure *Ag*(99.99%),*Cu*(99.99%)
supplied from Yemen Standardization Metrology and Quality Control Organization (YSMO) and pure *Sn*(99.99%) supplied from the scientific company of Yarmouk Company (YMK) Irbid, Jordan, these materials were weighed and mixed accurately. The mixture was melted in the engineering materials laboratory at the industrial engineering department - faculty of engineering - University of Jordan (JU) - Amman. the furnace used to melt the metals was preheated to 150 °C. The metals were put in ceramic crucibles, melt inside the furnace at 250 °C and then left to cool slowly to Room Temperature (R.T) in order to obtain samples containing the fully precipitated phases. The samples have been annealed at 110 °C for 6 hour and then slowly cooled to R.T. This procedure allowed for a small amount of grain stabilization to occur and allowed transformation to be nearly completed. This step was performed before the structure examination, mechanical and thermal tests.

The samples were prepared from the cast ingots obtained and were rolled drawn into circular cross-section wires of 0.08 *mm* diameter and 50 *cm* length and then cut into 5 c*m* length. The obtained samples were used in systematic measurements to recognize the mechanical, thermal and microstructural properties of the selected solder alloys. The melting temperatures of the solders were determined using a DSC. Moreover, we will explain the methods and practical tools that have been used in the tensile tests.

**Table. (1). Chemical compositions and melting point of the tested lead-free solder alloys.**

| Symbol | Compositions | Melting point (°C) |
|---|---|---|
| **A** | Sn-3.5wt% Ag | 221.48 °C |
| **B** | Sn-3.5wt% Ag-0.5wt% Cu | 219.8 °C |
| **C** | Sn-3.5wt% Ag-1.0wt% Cu | 218.1 °C |
| **D** | Sn-3.5wt% Ag-1.5wt% Cu | 217.2 °C |
| **E** | Sn-3.5wt% Ag-2.0wt% Cu | 218 °C |

Calorimetry is a primary technique for measuring the thermal properties of materials to establish a connection between temperature and specific physical properties of substances and is the only method for direct determination of the enthalpy associated with the process of interest. Calorimeters are used frequently in chemistry , biochemistry, cell biology, biotechnology, pharmacology and recently, in nanoscience to measure thermodynamic properties of the biomolecules and nano-sized materials.

DSC is a thermal analysis apparatus measuring the changing of physical properties of a sample, along with temperature against time. In other words, the device is a thermal analysis instrument that determines the temperature and heat flow associated with material transitions as a function of time and temperature. During a change in temperature, DSC measures a heat quantity, which is radiated or absorbed excessively by the sample on the basis of a temperature difference between the sample and the reference material. Heat flux of DSC for sample in enclosed pan ($N_2$) and an empty reference pan ($N_1$) are placed on a thermoelectric disk surrounded by a furnace as shown in figures (1). The furnace is heated at a linear heating rate and the heat is transferred to the sample and reference pan through the thermoelectric disk. However, owing to the heat capacity of the sample, there would be a temperature difference between the sample and reference pans which is measured by area thermocouples. DSC is a thermal analysis technique in which the difference in the amount of heat required to increase the temperature of a sample and reference is measured as a function of temperature. Both the sample and reference are maintained at nearly the same temperature throughout the experiment. Generally, the temperature program for a DSC analysis is designed such that the sample holder temperature increases linearly as a function of time [6]. The reference sample should have a well-defined heat capacity over the range of temperatures to be scanned. The basic principle underlying this technique is that when the sample undergoes a physical transformation such as phase transitions, more or less heat will need to flow to it than the reference to maintain both at the same temperature. Whether less or more heat must flow to the sample depends on whether the process is exothermic or endothermic. For example, as a solid sample melts to a liquid, it will require more heat flowing to the sample to increase its temperature at the same rate as the reference [43-44]. This is due to the absorption of heat by the sample as it undergoes the endothermic phase transition from solid to liquid. Likewise, as the sample undergoes exothermic processes such as crystallization less heat is required to raise the sample temperature. By observing the difference in heat flow between the sample and reference, DSC are able to measure the amount of heat absorbed or released during such transitions. DSC may also be used to observe more subtle physical changes, such as glass transitions. It is widely used in industrial settings as a quality control instrument due to its applicability in evaluating sample purity and for studying polymer curing [6-7].

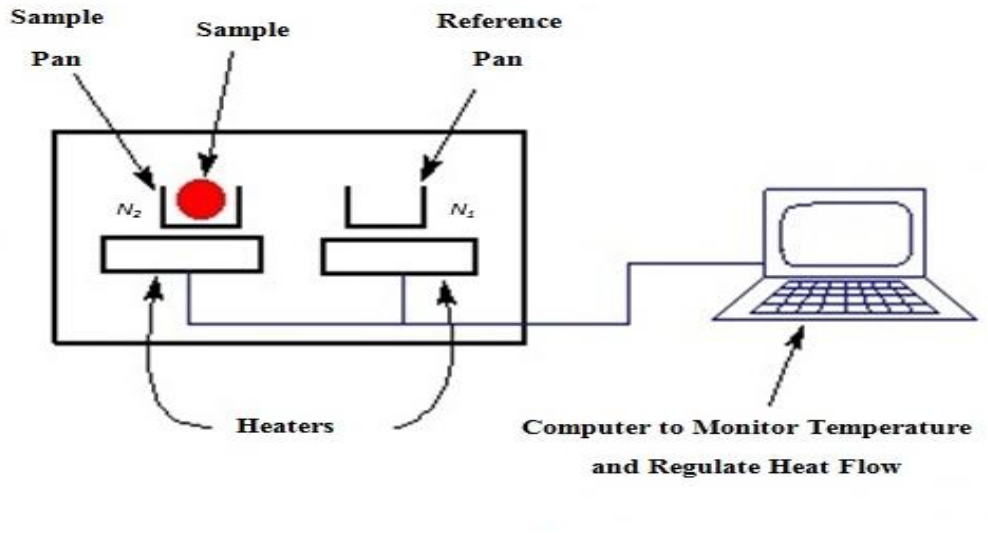


**Fig. (1). Diagram of DSC device.**

This analysis has been carried out in materials science laboratory at the physics department - faculty of science - University of Jordan – Amman. Small samples from each alloy, less than 15 *mg* was placed in high-purity aluminum pans ($N_2$), then closed by a custom. The sample pans and an empty high-purity aluminum pans ($N_1$) are placed in protective atmosphere. In the present work, the Melting Temperature ($T_m$) of the five solder alloys were estimated with DSC brand (*NETZSCH-DSC 200 F3*). The samples were initially scanned from 20 to 300 °C at heating rate of 10.0 (°C/min) in order to analyze the thermal properties of investigated samples. Pure *Sn* was used as a standard material. In addition, for each DSC curve, its area under the curve was integrated with available software to calculate the fusion heat of each solder alloy.

## 1:Preparation of Metallographic Samples

### 1-1:Mechanical Polishing

For producing a surface which is scratching free and surface like mirror, mechanical polishing was used often done in two stages, with a coarse stage and a fine abrasive or polishing agents, respectively.

### 1-2:Chemical Etching

Specimen should be washed free of any adhering polishing compound and then rubbed from the sides of the specimen with cotton, keeping the polished face clean. Even now the specimen may be slightly greasy, the best way to remove grease is immersion wire samples with ethanol $C_2H_5OH$ for about two minutes. The specimens has been removed from the ethanol $C_2H_5OH$ and immersion in running water before being etched.

For the observation of the interface microstructure the solder joints were etched slightly by using *5% HCl – 95%* $C_2H_5OH$ solutions for 5-10 seconds after mechanical cutting and polishing. the solders on substrates were etched deeply by using *10% HCl – 90%* $C_2H_5OH$ solution for 5-10 seconds followed by etching by *10%* $HNO_3$ *– 90%* $C_2H_5OH$ solution for 5-10 seconds.

## 2:Tensile Testing Procedure

Tensile stress –strain and compressive creep tests have been performed on all samples at different temperatures from 40 to 100 °C and two different loads of 9.8 and 11.76 MPa, using a horizontal tensile technique. A schematic drawn of apparatus is shown in figure (2) and figure (3), which is essentially the same as that described, by

compressive creep test apparatus. This system consists of four parts: (i) uniform hot zone (furnace), (ii) specimen zone, (iii) gauge length, (iv) loading weight (that the load is applied axially to the specimen). The sample was placed between fixed and mobile arm inside the furnace, the load was put on the lever arm and appropriate temperature was setting. The sample has been subjected to a horizontal elongation which is recorded by gauge length and the time is determined by digital clock stopped. All the components of the stress-strain machine has been designed in materials science laboratory at the physics department of the faculty of science - Sana'a University - Yemen and constructed especially to be more suitable for soft alloys measurements.

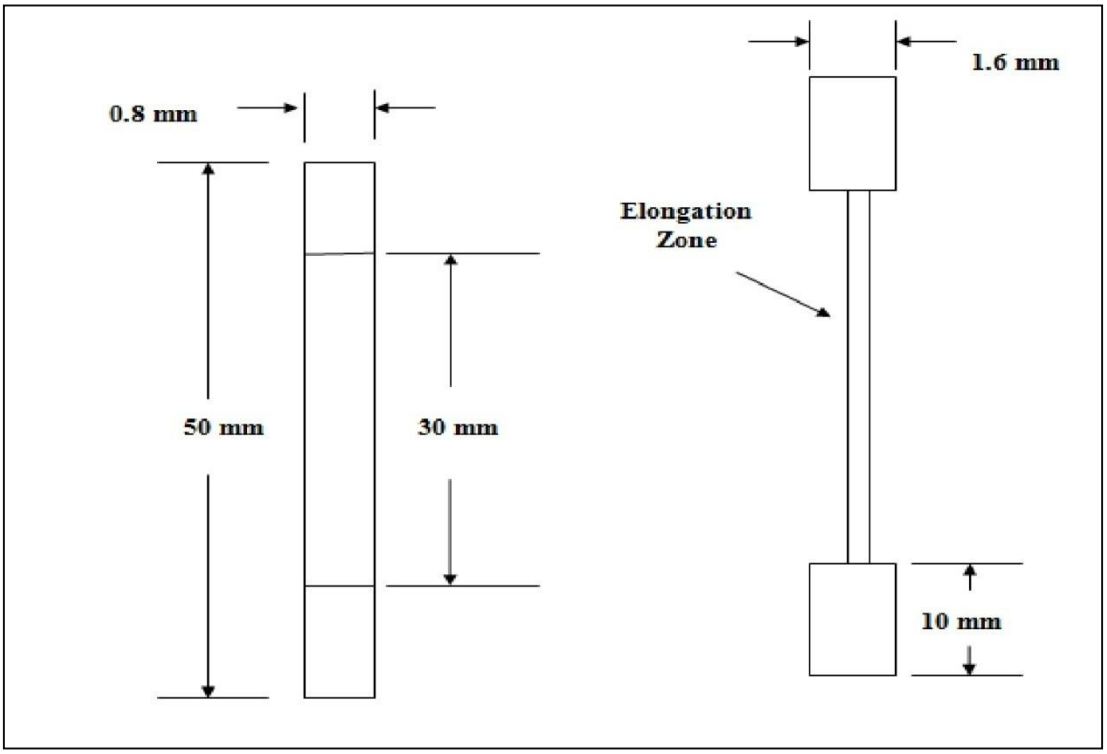


**Fig. (2). Diagram of a specimen geometry.**

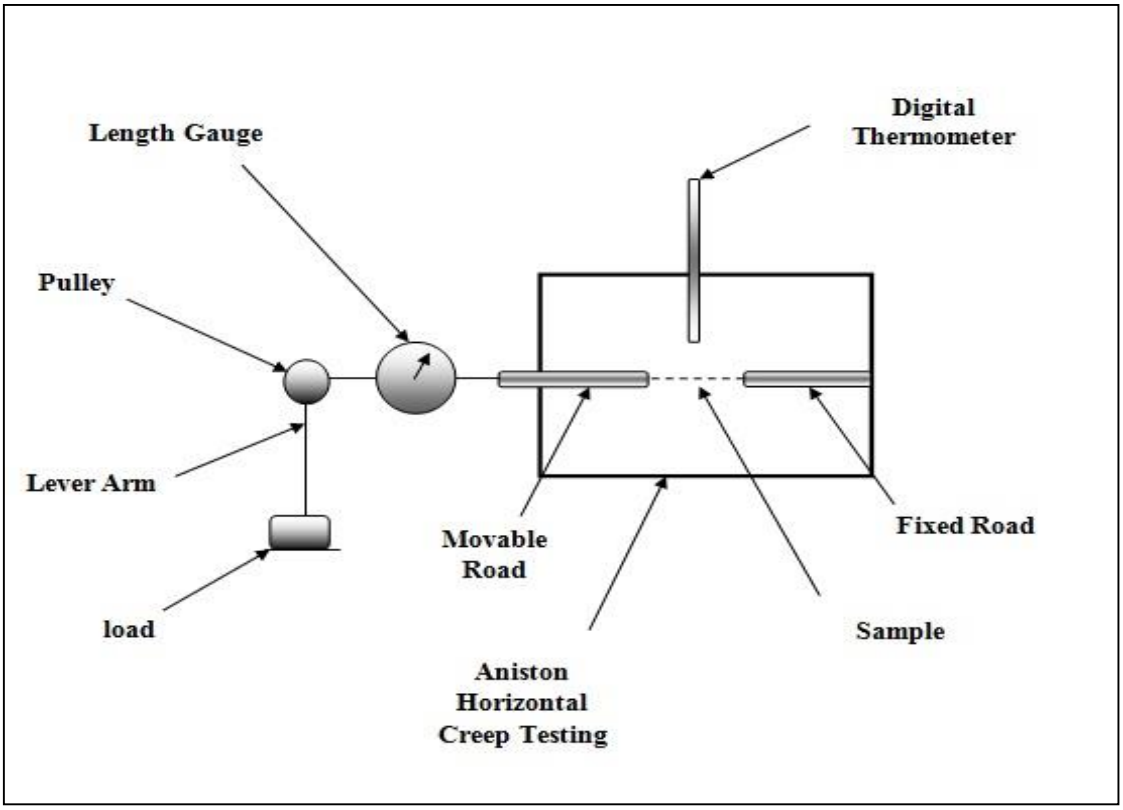


**Fig. (3). Diagram of horizontal creep testing machine.**

## Results and Discussion:

This study discussed and compared the results of thermal analysis of the five solder alloys as a function of Cu-containing. Thermal analysis includes discussion of DSC curve, estimating the melting point, comparing the results of selected alloys and other alloys, measuring the pasty range and calculating the heat of fusion for tested solder alloys is also represented in this chapter. Typical creep curves from *A* to *E* alloys are presented and of the isothermal tensile creep characteristic are discussed for the solder alloys as function of strain rate and testing temperature.

## 1:Thermal Properties

The fundamental thermal behaviors of eutectic solder alloys *A* and from *B* to *E* alloys were analyzed using DSC. The result of the analysis are shown in figures (4 a, b, c, d and e). The melting point of the alloy was determined from the heating portion of the DSC cycle, using the following convention. First, a ‘‘baseline’’ was constructed under the transformation peak. Then, a second line was constructed at the inflection point of the leading edge of the transformation peak, having the same slope as that of the trace at the inflection point. The melting point was designated by the intersection between the latter line and the baseline as shown in figure (5). Because the objective of the present study required that a large number of alloy variations be explored, the exact determination of the melting point was omitted in favor of a qualitative assessment based upon the shape and width of the transformation [8-10].

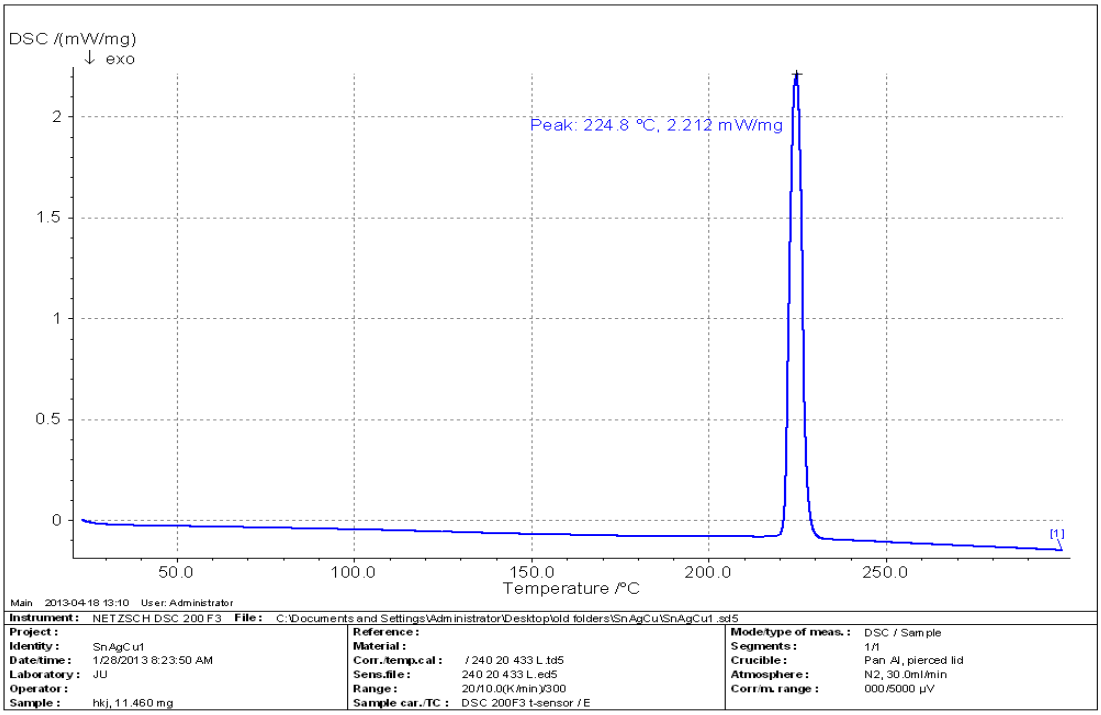


**Fig. (4a). DSC thermogram of the *A* solder.**

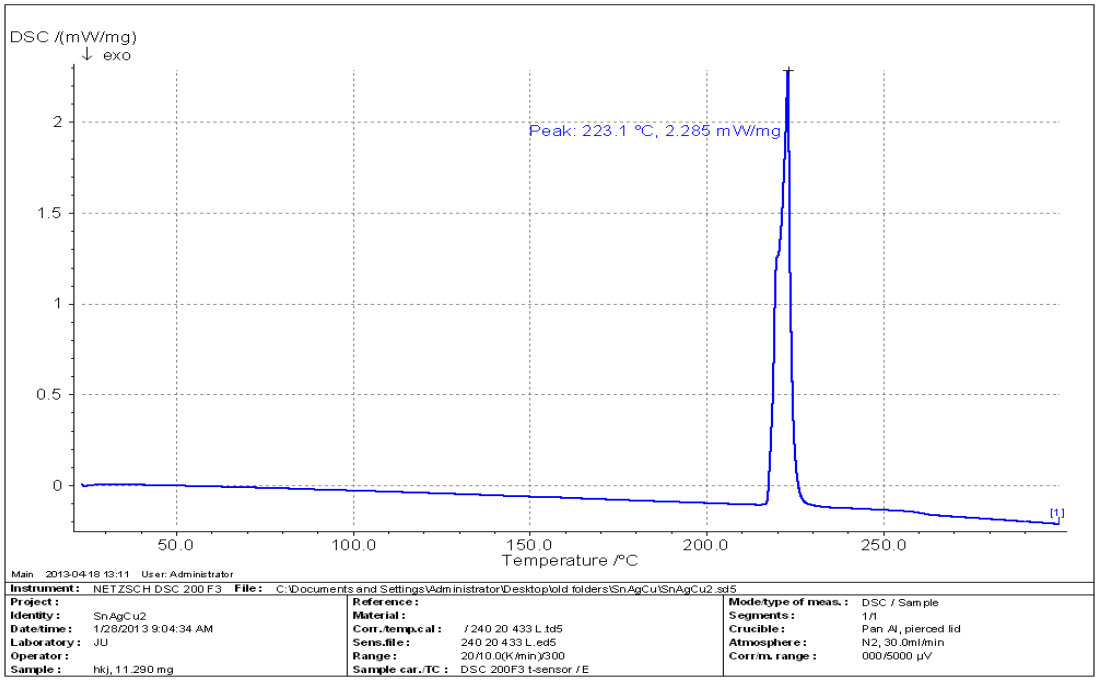


**Fig. (4b). DSC thermogram of the *B* solder.**

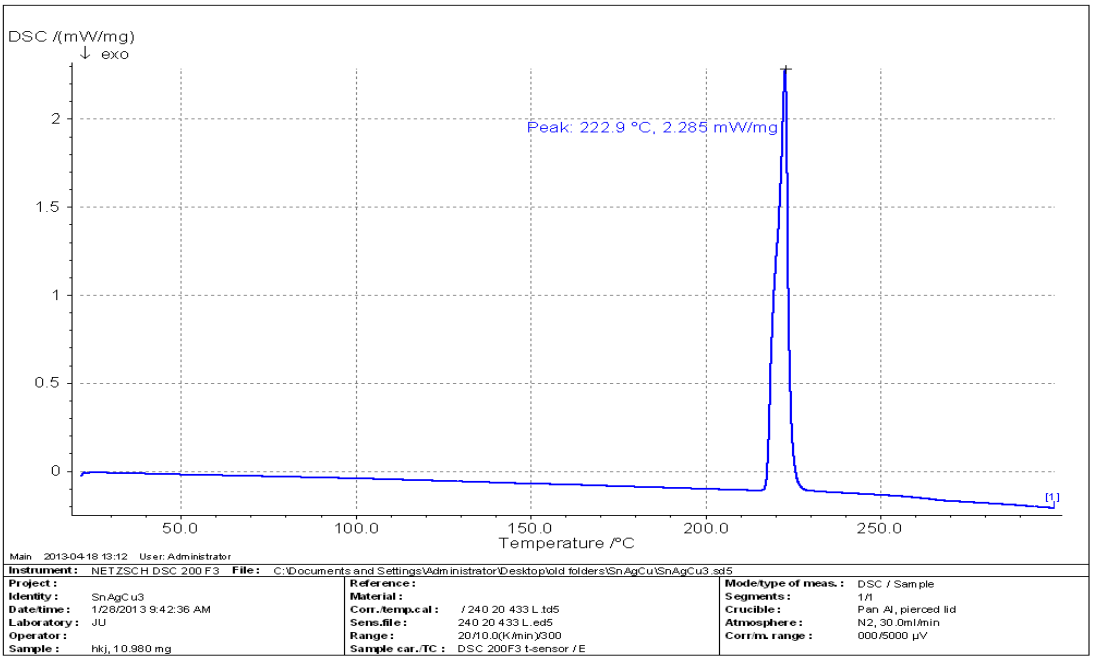


**Fig. (4c). DSC thermogram of the *C* solder.**

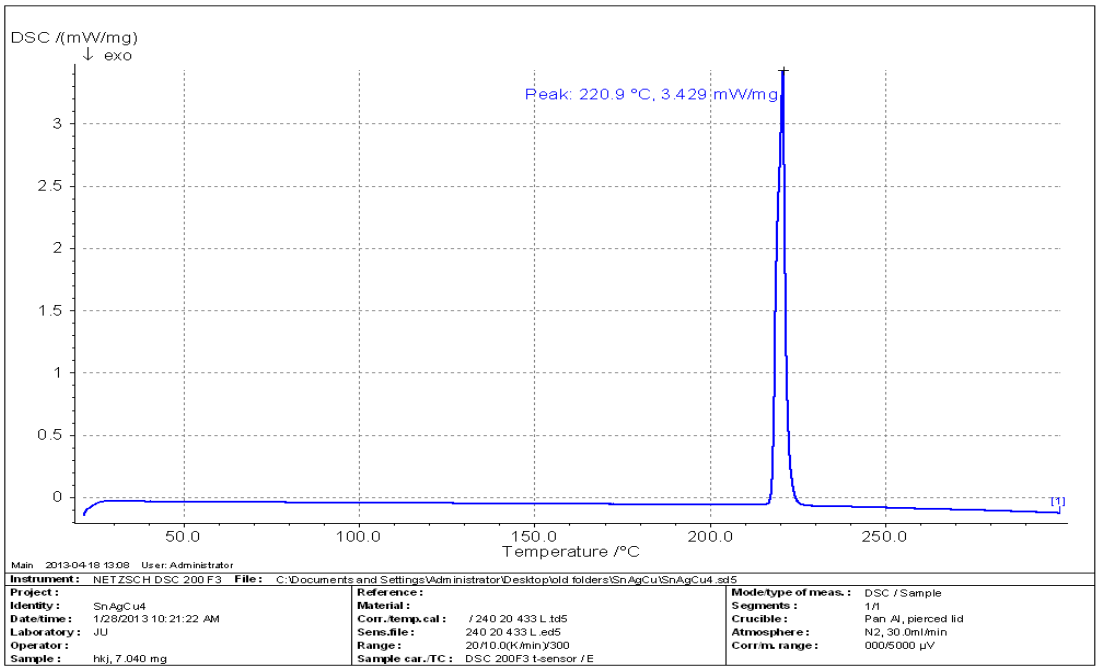


**Fig. (4d). DSC thermogram of the *C* solder.**

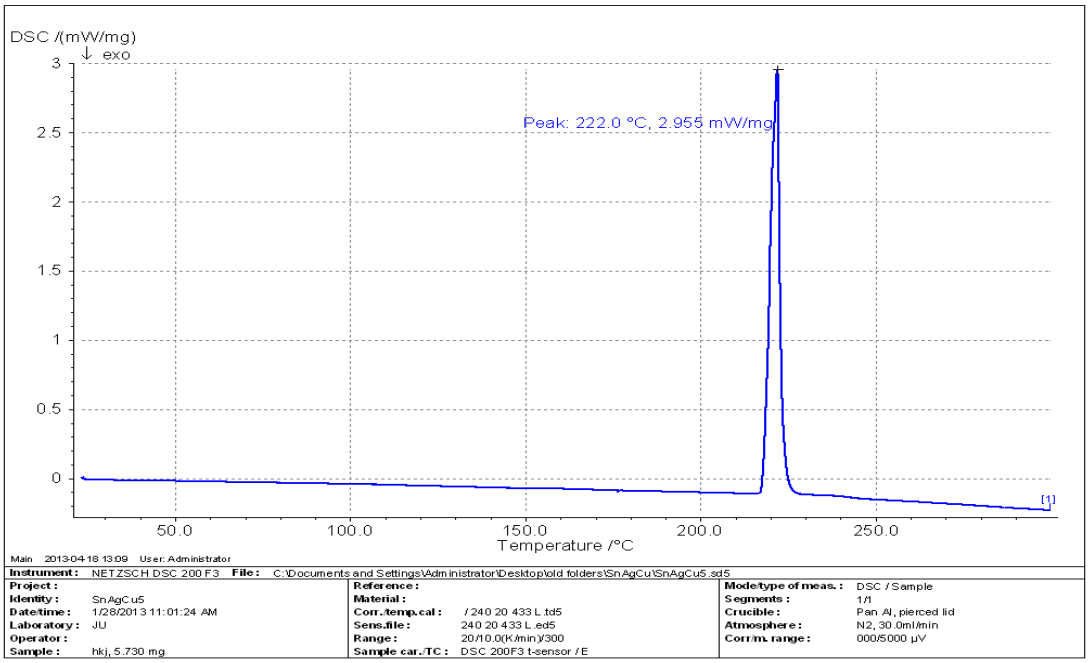


**Fig. (4e). DSC thermogram of the *D* solder.**

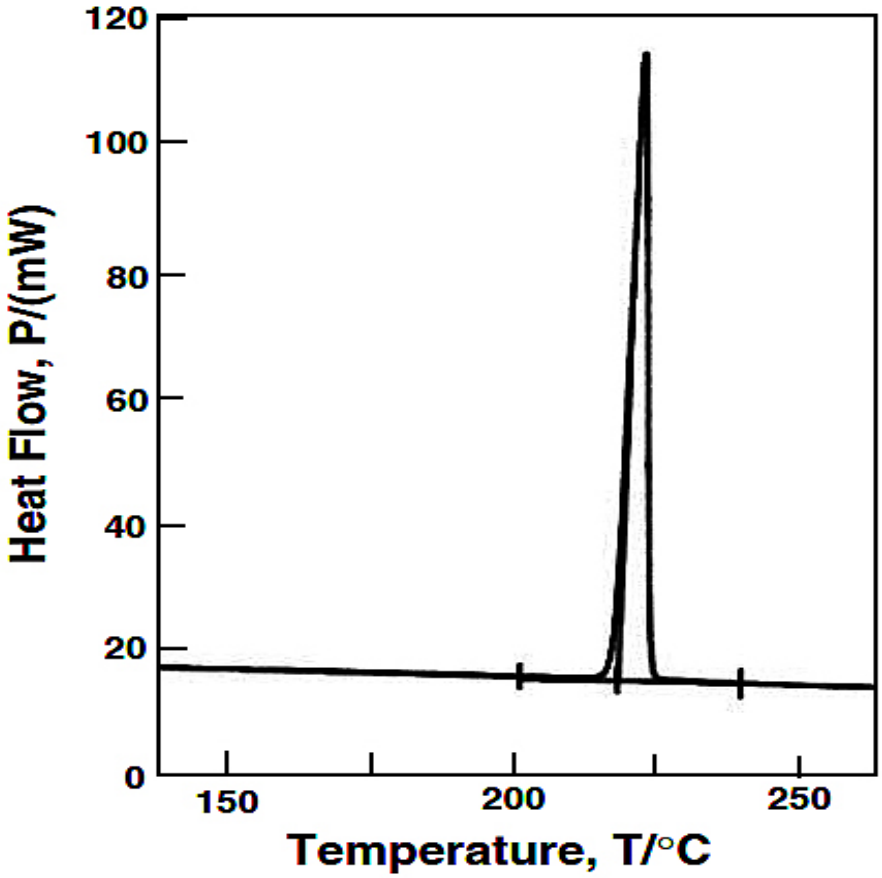


**Fig. (5). Diagram to set melting point [8].**

**Table. (2). Comparison between solidus temperature $T_{onset}$ , liquidus temperature $T_{end}$ , melting point and heat of fusion ($\Delta H$) for the various solder alloys.**

| Compositions | $T_{onset}$ (°C) | $T_{end}$ (°C) | Pasty Range (°C) | Melting Point $T_{end}$-$T_{onset}$ (°C) | Heat of Fusion ΔH (J/g) |
|---|---|---|---|---|---|
| **A** | 219.9 | 229.8 | 9.9 | 221.48 | 195.69 |
| **B** | 217.2 | 226.4 | 9.2 | 219.8 | 193.73 |
| **C** | 217.0 | 226.0 | 9 | 218.1 | 200.41 |
| **D** | 216.7 | 224.5 | 7.8 | 217.2 | 344.10 |
| **E** | 216.6 | 225.0 | 8.4 | 218 | 417.14 |

The DSC results are summarized in table (2). As a small amount of Cu element was added, the eutectic melting point of *A* changes significantly. The melting point alloy 219.8, 218.1, 217.2 and 218 °C from the *B* to E respectively, as compared with 221.48 °C for A eutectic alloy.

With the addition of small amount of *Cu* element, melting point of *A* changed only slightly. The eutectic temperatures were 219.8, 218.1, 217.2 and 218 °C for the *B, C, D* and *E* respectively, as compared with 221.48 °C for *A* eutectic alloy. On the other hand, the eutectic *Sn–3.5Ag* alloy (*B-E*) exhibited additional change in the liquidus ($T_{onset}$) and solidus ($T_{end}$) temperatures. The ($T_{onset}$) and ($T_{end}$) decreased in these ternary alloys, as can be seen from table (2).

The pasty range value, which is the difference between the ($T_{end}$) and ($T_{onset}$) temperatures is very important in electronic soldering and other industrial applications. We found that the measured pasty range ($T_{end} - T_{onset}$) decreased from 9.2°C to 8.4°C which is lower than 9.9 °C for *A* eutectic.

The heat of fusion ($\Delta H$) can be determined by the following equation:

$$\Delta H = K_H A_H / m_H , \qquad (1)$$

where ($K_H$) is a constant with the value of 2.64 for pure tin, ($m_H$) is the mass of the sample and ($A_H$) is the area under the endothermic peak [11-15]. The values of $\Delta H$ obtained for different solders are 193.73, 200.412, 344.1, 417.143 and 195.69 J/g for the *A* eutectic, *B, C, D* and *E* alloys, respectively, showing that less energy is necessary to be consumed for melting the solder alloys. It is obvious that the fusion heat of *E* is larger than that of the Composition *A* eutectic, where as *B* the present ternary solder alloys exhibits the lowest one, which indicates that the *A* and *B* alloys are considered as the most beneficial material for saving energy.

## 2: Mechanical Properties

### 2-1:Comparative Strain-Time Curves

The strain behavior of *A* to *E* alloys under different stresses and temperatures has been carried out by plotting strain with time at (i) different temperatures and constant load of 9.8 and 11.76 MPa and (ii) different loads and constant temperature 40 °C, 70 °C and 100 °C as shown in figures (6 a, b, c, d, e and f) and table (3).

All carves in figures (6 a-f) show three stags, primary stage, secondary stage and tertiary stage. The primary region is characterized by transient creep with decreasing creep rate,

$$\dot{\varepsilon} = \mathbf{A}\left(\frac{\sigma}{E}\right)^{n} e^{\left(-\frac{Q}{RT}\right)} . \qquad (2)$$

Clearly this elongation increases with stress and temperature [11-15]. On the other hand, elongation increased with the addition of small amount of *Cu* element and increasing temperature and loads, as shown in figures (6 a, b, c, d, e and f) and table (3).

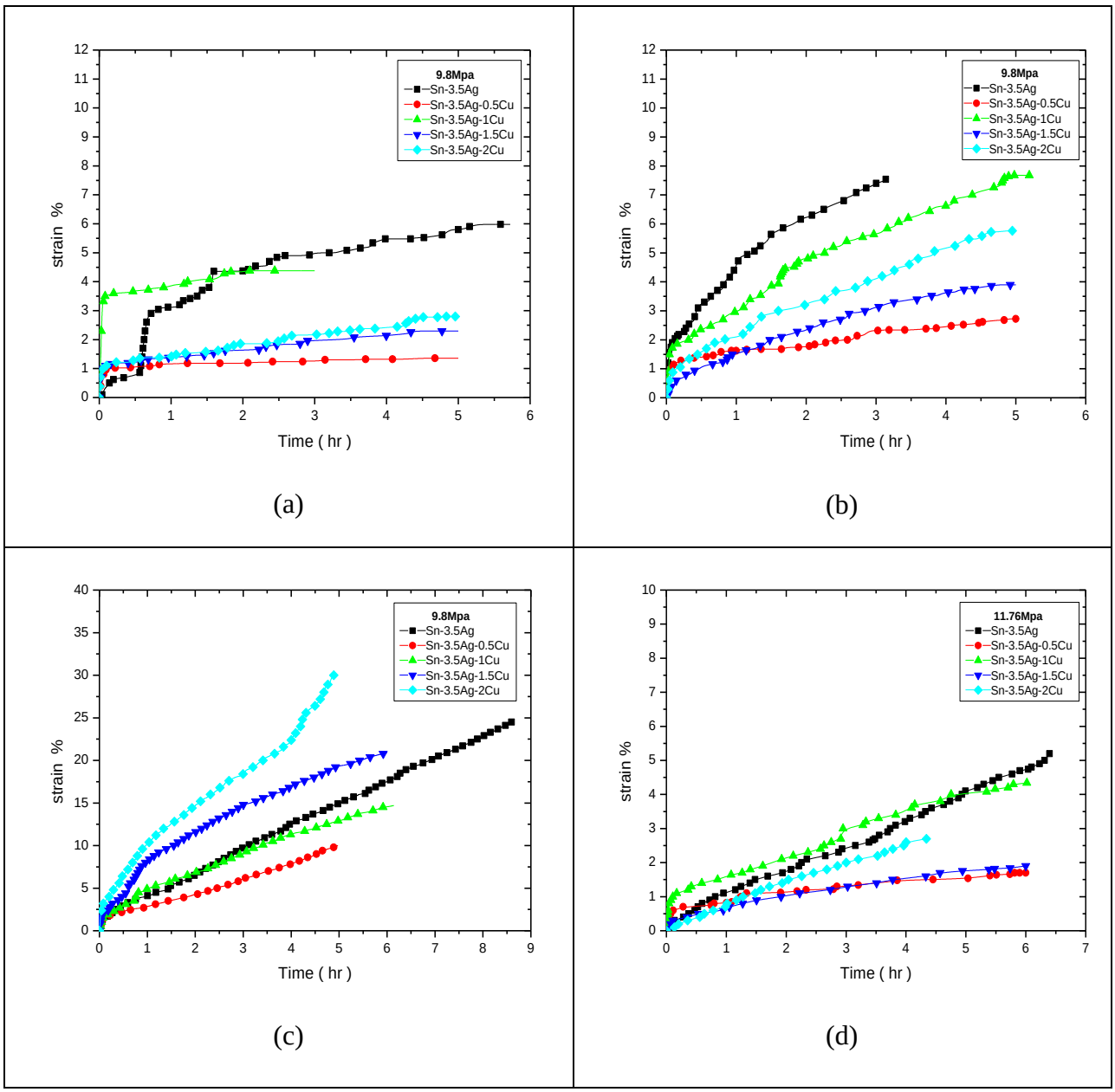

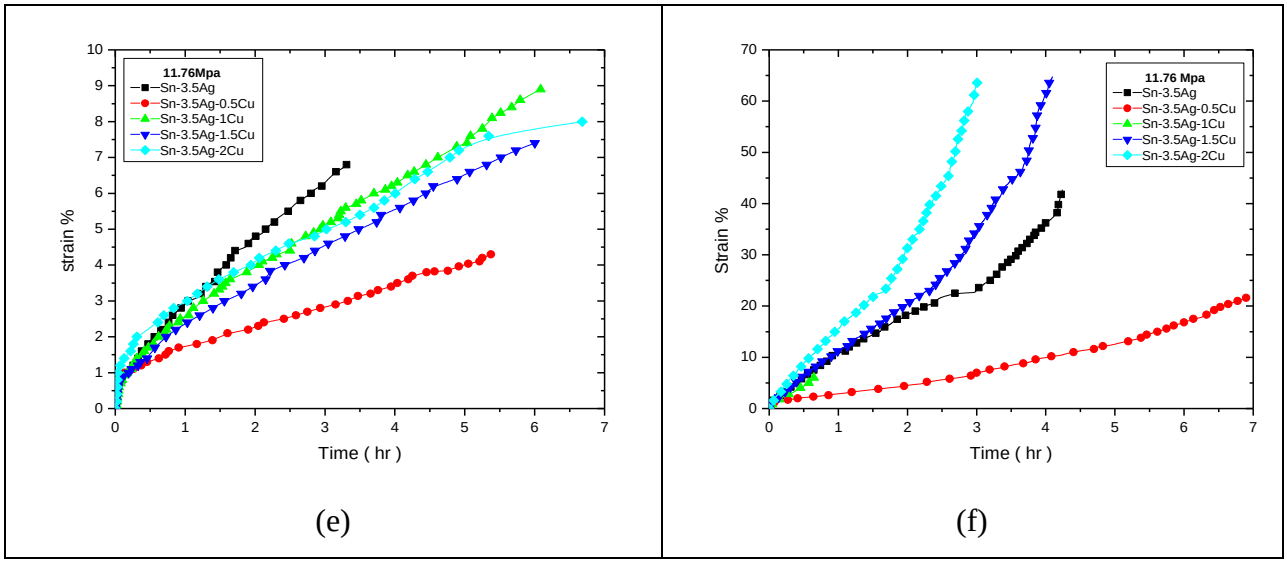


**Fig. (6). Strain-Time curves for solder alloys at temperature 40,70,100°C and stress 9.8, 11.76 MPa.**

| Compositions | Elongation % | | |
|---|---|---|---|
| | Temp (°C) | 9.8 MPa | 11.76 MPa |
| A | 40 | 1.99 | 2.56 |
| | 70 | 3.72 | 3.4 |
| | 100 | 12.24 | 21.25 |
| B | 40 | 0.63 | 0.83 |
| | 70 | 1.29 | 2.1 |
| | 100 | 4.9 | 10.9 |
| C | 40 | 1.1 | 2.08 |
| | 70 | 3.75 | 4.4 |
| | 100 | 7.74 | 7.07 fracture composition |
| D | 40 | 1.35 | 0.93 |
| | 70 | 1.94 | 3.65 |
| | 100 | 10.35 | 32.3 |
| E | 40 | 2.94 | 1.3 |
| | 70 | 2.87 | 3.9 |
| | 100 | 14.25 | 31.9 |

**Table. (3). The elongation % at different temperatures form 40,70 and 100 °C and at stress of 9.8 and 11.76 MPa.**

## 2-2: Comparative Steady-State Creep Curves

The study of the creep behavior of solder joints will be more representative, as it mimics the practical service conditions. It is well established that during soldering, the dissolution of the substrate into the solder and the solder consumption resulted by the diffusion of the solder alloy constitutions into the interface and substrate can influence the microstructure of the solder, which in turn will affect the property of the material [16-19].

Typical creep curves of the *Sn-Ag-Cu* alloys are presented as shown in figures (7 a, b and c). The materials showed characteristics of the secondary creep stage immediately after load were applied with short primary creep stage. It appears that the hardening of the matrix with the creep strain was recovered immediately because of the high temperature and different loads. Effects of *Cu* additions on the creep curves are presented.

The creep results showed that *Sn-Ag-Cu* solders which containing a small amount of *Cu* element exhibited significantly improved creep resistance and creep time to failure. Figures (7 a-c) show the steady-state creep rates of *A* to *D* solders. The improvement in creep resistance can be attributed to the presence of *Cu* which aids to resist the motion of the dislocations. From figures (7 a-c), it was also noted that at the highest applied temperatures level of 100 °C and of applied stress level of 9.8 and 11.76 MPa, the steady-state creep rate was observed to be higher as comparing that at 40 °C and 70 °C. Also (3) showed the stress exponent (*n*) and the strain rate sensitivity (m) of the monolithic and composite solder joints under testing temperatures of 40 °C, 70°C and 100°C and applied stress of 9.8 and 11.76 MPa.

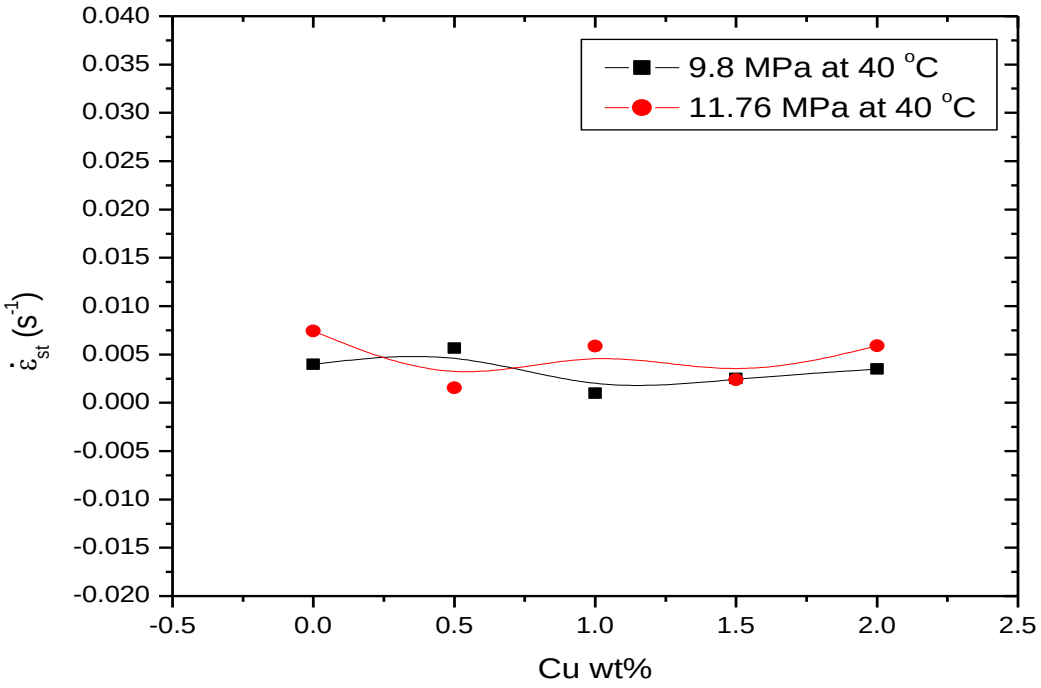


**Fig. (7 a). Steady-State creep rate as a function of *Cu* concentration of the solder alloys subjected to 9.8 MPa and 11.76 MPa at 40 °C.**

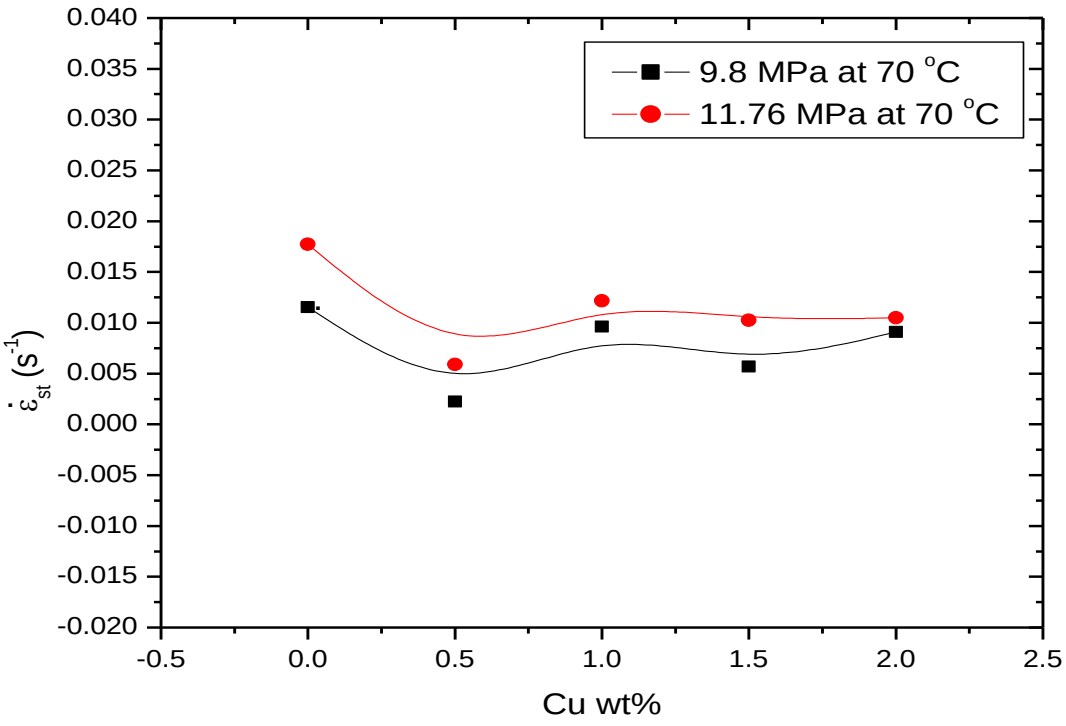


**Fig. (7 b). Steady-State creep rate as a function of *Cu* concentration of the solder alloys subjected to 9.8 MPa and 11.76 MPa at 70 °C.**

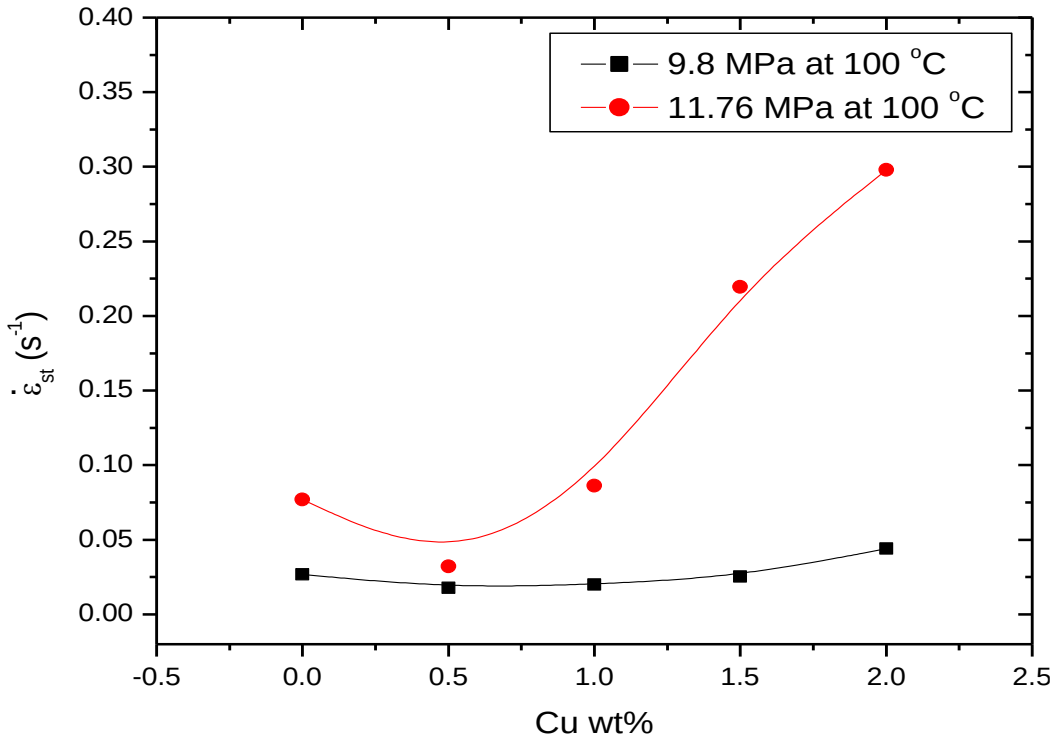


**Fig. (7 c). Steady-State creep rate as a function of *Cu* concentration of the solder alloys subjected to 9.8 MPa and 11.76 MPa at 100 °C.**

The results in general showed that the (*n*) values of composite solders were higher than that of the monolithic *A* solder. This observation was particularly evident in the high stress regime as shown in figures (7 a, b and c), this could be attributed to the effect of *Cu* addition in the solder matrix. Addition of *Cu* influenced the distance for which dislocations glide between the reinforcements and also the forces that caused them to climb and by-pass the reinforcements. This observation is consistent with those reported by investigators [20-21], working on tin-based solder alloys from *A* to *E*. Such precipitation-strengthened alloys also have higher (*n*) values than those obtained in pure tin, due to the presence of intermetallic second phases.

The (*n*) values decreased significantly with increasing applied stress and with increasing testing temperature. This signified that the reinforcement strengthening effect was greater at lower testing temperature and high stress regime. Furthermore, creep resistance was more evident at low testing temperatures.

Table (4) and figures (8 a-c) show the strain rate sensitivity (*m*) at different temperatures of the *A* eutectic, *B, C, D* and *E* alloys.

**Table. (4). The stress exponent (*n*) strain rate sensitivities (*m*) of solder alloys.**

| Compositions | n | | | m | | |
|---|---|---|---|---|---|---|
| | 40 (°C) | 70 (°C) | 100 (°C) | 40 (°C) | 70 (°C) | 100 (°C) |
| **A** | 2.21 | 1.79 | 1.3 | 0.45 | 0.56 | 0.77 |
| **B** | 2.45 | 2.38 | 1.58 | 0.41 | 0.42 | 0.63 |
| **C** | 2.06 | 1.91 | 1.36 | 0.49 | 0.52 | 0.74 |
| **D** | 2.54 | 2.06 | 1.12 | 0.39 | 0.49 | 0.89 |
| **E** | 2.48 | 1.96 | 0.95 | 0.40 | 0.51 | 1.05 |

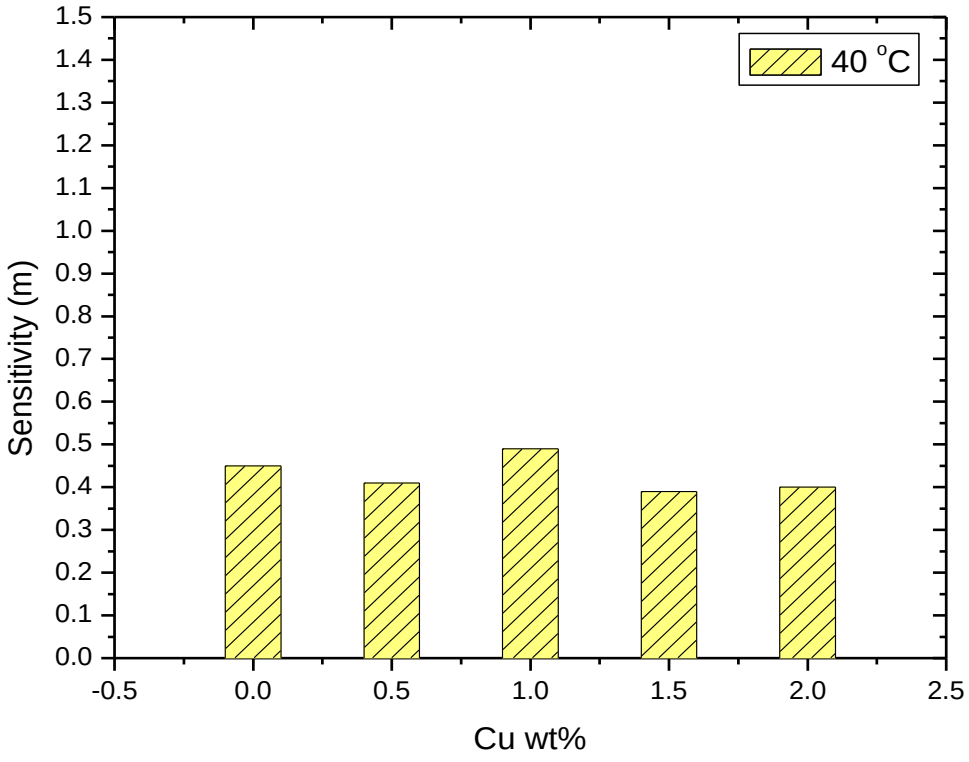


**Fig. (8 a). The strain rate sensitivity (*m*) as a function of *Cu* concentration for *A* to *E* solder alloys at 40 °C.**

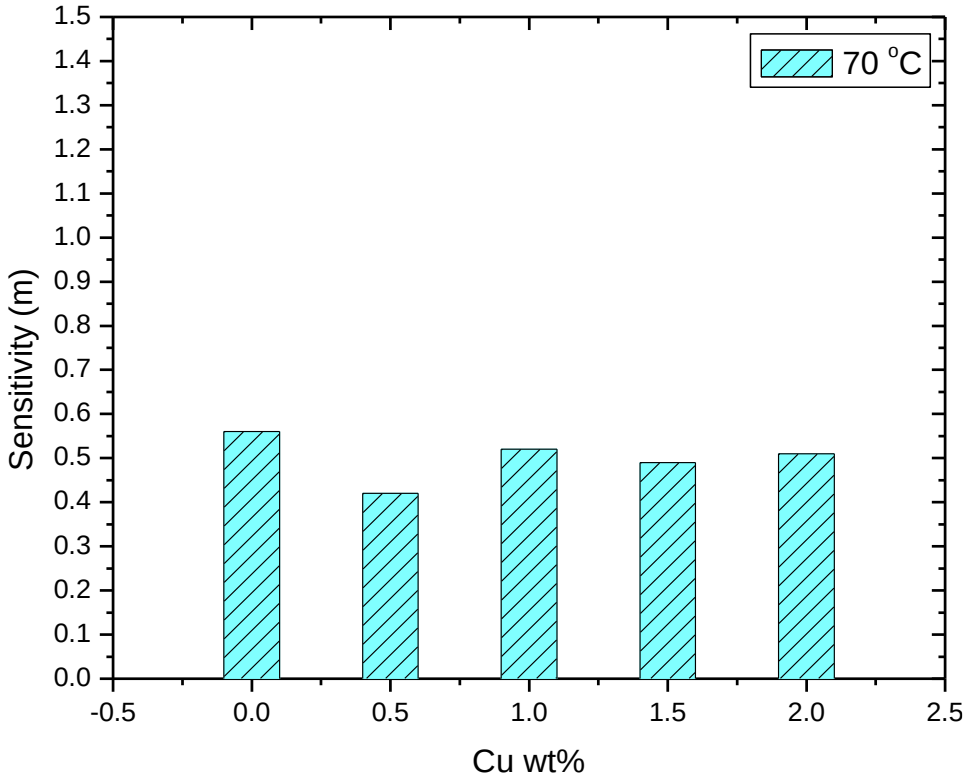


**Fig. (8 b). The strain rate sensitivity (*m*) as a function of *Cu* concentration for *A* to *E* solder alloys at 70 °C.**

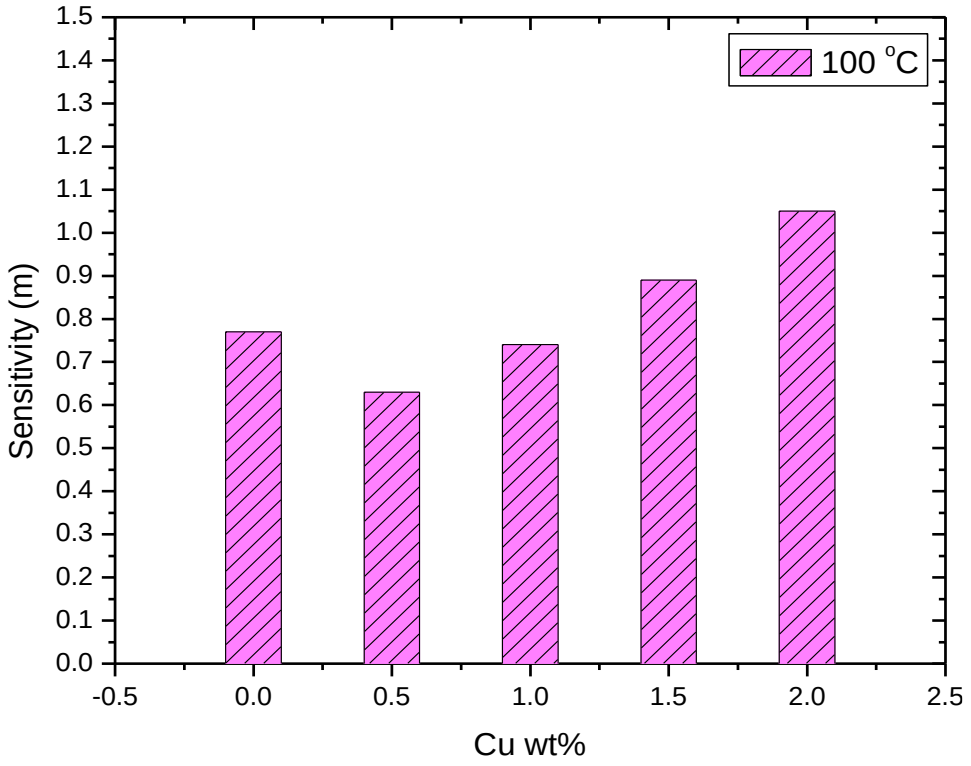


**Fig. (8 c). The strain rate sensitivity (*m*) as a of *Cu* concentration for *A* - *E* solder alloys at 100 °C.**

## 2-3 : Activation Energy of Lead-Free Solder Alloys

Activation energy of creep is described as the energy barrier that is needed for an atom to move from a high energy location to a lower energy location. The activation energies (*Q*) of creep at the stress regimes were determined by Eq:

$$\mathbf{Q} = -\mathbf{R}\left[\frac{\partial \ln \dot{\varepsilon}}{\partial(1/T)}\right]_{\sigma} \qquad \textbf{(3)}$$

figure (9 a, b, c, d, e) shows the computation of creep activation energy values of the monolithic *Sn-Ag-Cu* solder joints under different stresses. With the addition of small amount of *Cu* element, the activation energies changed clearly, decreased for *A, B* alloys and increased for *C,D* alloys. Also It was observed that the activation energies were stress dependent for each solder system 9.8 MPa, 11.76 MPa. This higher activation energy values for *Sn-3.5Ag1.5Cu wt%* at 11.76 MPa is consistent with its greater creep resistance, when compared to *Sn-Ag-Cu* alloys, and higher activation energy values for *Sn-3.5Ag2.0Cu* at 9.8 MPa, when compared to *Sn-Ag-Cu* alloys as shown in table (5). In essence, the results revealed that the addition of reinforcement in *Cu* improves the creep resistance of the *Sn-Ag-Cu* alloys, the improvement in creep resistance can be attributed to the presence of *Cu* which aid to resist the motion of the dislocations [21].

In light of earlier established results, the creep results of the present study further demonstrated that composite technology in electronic solders can lead to simultaneous improvement in: (i) thermal performance (in terms of lower melting point and melting temperature) and (ii) mechanical performance (tensile, elongation and creep properties).

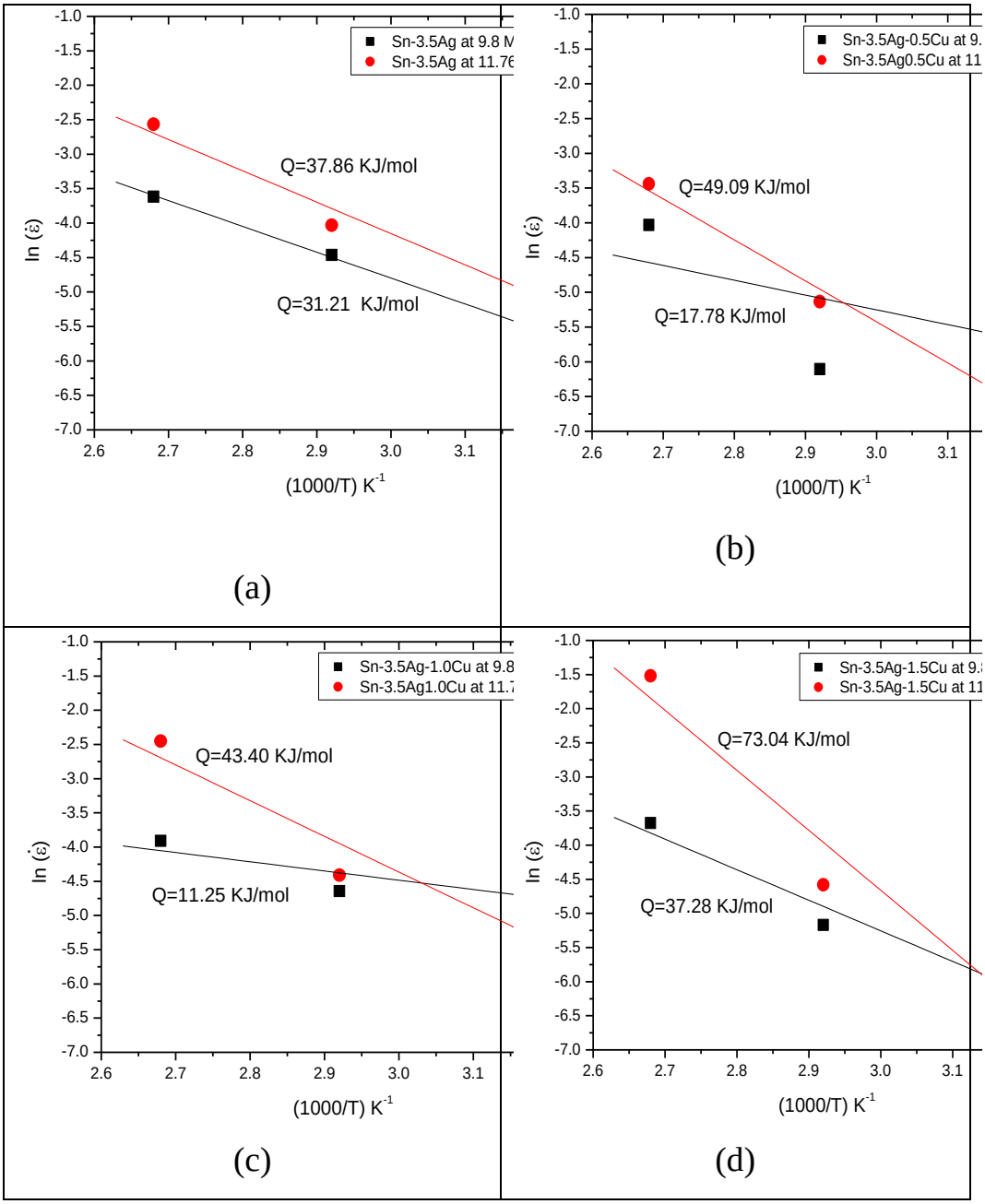
Sn-3.5Ag at 9.8 M
Sn-3.5Ag at 11.76
Q=37.86 KJ/mol
Q=31.21 KJ/mol
ln (ε̇)
(1000/T) K-1
(a)
Sn-3.5Ag-0.5Cu at 9.
Sn-3.5Ag0.5Cu at 11
Q=49.09 KJ/mol
Q=17.78 KJ/mol
ln (ε̇)
(1000/T) K-1
(b)
Sn-3.5Ag-1.0Cu at 9.8
Sn-3.5Ag1.0Cu at 11.7
Q=43.40 KJ/mol
Q=11.25 KJ/mol
ln (ε̇)
(1000/T) K-1
(c)
Sn-3.5Ag-1.5Cu at 9.
Sn-3.5Ag-1.5Cu at 11
Q=73.04 KJ/mol
Q=37.28 KJ/mol
ln (ε̇)
(1000/T) K-1
(d)

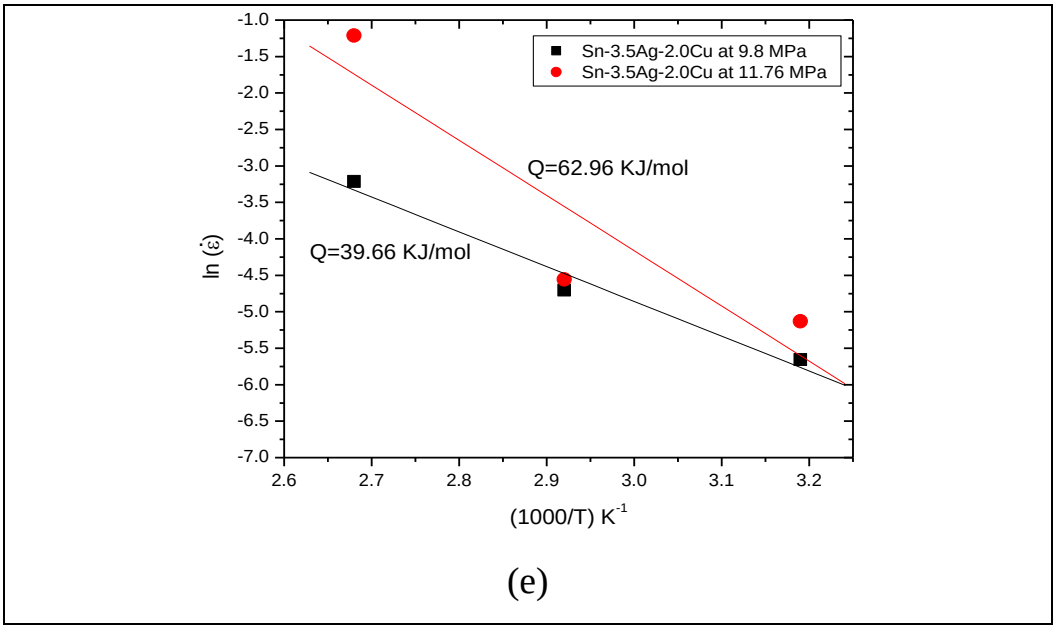


(e)

**Fig. (8). Creep activation energy (*Q*), A to E solder joints under different stresses.**

**Table. (5). Activation energy of soldering alloys at load 9.8, 11.76 MPa.**

| Composition | Load (MPa) | Activation Energies (Q) (KJ/mol) |
|---|---|---|
| **A** | 9.8 | 31.21 |
| | 11.76 | 37.86 |
| **B** | 9.8 | 17.78 |
| | 11.76 | 49.09 |
| **C** | 9.8 | 11.25 |
| | 11.76 | 43.40 |
| **D** | 9.8 | 37.28 |
| | 11.76 | 73.04 |
| **E** | 9.8 | 39.66 |
| | 11.76 | 62.96 |

## Conclusions:

The effect of separate and dual additions of small amount of *Cu* on the structure and mechanical properties as well as thermal behavior of the *A* eutectic solder alloy has been investigated . The results are summarized as follows:

1. The addition of copper, has been decrease the melting temperature, melting point and solidus temperature besides broadening the pasty range and increasing heat of fusion. These characteristics is very important in electronic soldering and other industrial applications.
2. For all tested SAC family alloys, the elongation increased with increasing temperature, an load and also by adding *Cu*. The ductility changes were generally large for *C* and *D* lead-free solder.
3. The creep results showed that *Sn-Ag* solders which containing *Cu* exhibited significant improvement in creep resistance and increased creep time to failure. the improvement in creep resistance can be attributed to the addition of *Cu* which aid to resist the motion of dislocations.
4. The strain rate sensitivities at different temperature of the *A* eutectic and other alloys were different. The (*m*) value is remarkably larger for *E* then the other lead-free solder alloys at 100 ℃ and *A* eutectic at 70°C and *C* at 40 °C.
5. The range of activation energy values of *A* eutectic was found to be comparable to that of monolithic SAC. However at different system loads from 9.8 to 11.76 MPa, the range of activation energy values different accordingly.
6. The *SAC* lead-free solder proved to be promising in that it gave good combination specifications than the other four alloys, the best alloys which contain from 0.5 to 1.0 *wt% Cu* which was possible due to the formation of hard, soft $Ag_3Sn$ and $Cu_6Sn_5$ precipitates.

## References:


[1]. **Wu, C.M.L.; Yu, D.; Law, C. M. T.; and Wang, L.**; J. Mater. Sci. Eng.R, vol. 44 (2004) pp.1-44.
[2]. **McCabe, R. J**.; PhD. Thesis; Northwestern unv., (**2000**) p.3.
[3]. **Massalski, T.B.**; "Binary Alloy Phase Diagram", ASM International,
2ed. vol.3 (1990) pp. 2573-2574.
[4]. **Turbini, L. J.; Munie, G. G.; Bernier, D.; Gamalski, J. and Bergman,D.;** Electron. Packag. Manufact., IEEE Transactions; vol. 24
(2001) pp. 2-3.
[5]. **Moon, K.W. and Boettinger, W. J.;** JOM, vol. 56 (**2004**) pp. 22-
[6]. **Abtew, M.; and Selvaduary, G.;** J. Mater. Sci. Eng. R, vol. 27 **(2000)**
pp. 95-141.
[7]. **Lin LN, Mason AB, Woodworth RC, Brandts JF**. Calorimetric studies of the N-terminal half-molecule of transferrin and mutant forms modified near the Fe(3+)-binding site. Biochem J 1993.
[8]. **Protasevich I, Ranjbar B, Lobachov V, et al. Conformation and thermal denaturation of apocalmodulin**: role of electrostatic mutations. Biochemistry 1997.
[9]. Paul Vianco, **Jerome Rejent and Richard Grant**. Sandia National Laboratories, Albuquerque, NM 87185, USA.
[10]. **Weber PC, Salemme R. Applications of calorimetric methods to drug discovery and the study of protein interactions**. Curr Opin Struc Biol 2003.
[11]. **Haynie DT. Biological Thermodynamics**. Cambridge, UK: Cambridge University Press, 2008.
[12]. **Haines PJ, Reading M, Wilburn FW. Differential thermal analysis and differential scanning calorimetry**. In Brown ME, editor. (ed): Handbook of Thermal Analysis and Calorimetry, vol 1 The Netherlands: Elsevier Science BV.
[13]. **Danley RL. New heat flux DSC measurement technique**. Thermochim Acta 2002.
[14]. **Zucca N, Erriu G, Onnis S, Longoni A**. An analytical expression of the output of a power-compensated DSC in a wide temperature range. The rmochim Acta 2002.
[15]. **Dean , John A. The Analytical Chemistry Handbook**. New York: McGraw Hill , (1995).

[16]. **Varghesea N, Vivekchanda SRC, Govindaraja A, Rao CNR**. A calorimetric investigation of the assembly of gold nanorods to form necklaces. Chem Phys Lett 2008.
[17]. **Z. G. Chen, Y. W. Shi and Z. D. Xia**, J. Electron. Mater. **33** (9), 964 – 971 (2004).
[13]. **F. G. Yost, F. M. Hosking and D. R. Frear**, in: The Mechanics of Solder Alloy Wetting and Spreading, New York, Van Nostrand Reinhold (1993).
[18]. **F. Guo F, J. Lee, J. P. Lucas, K. N. Subramanian and T. R. Bieler, J.** Electron. Mater. **30** (9), 1222 - 1227 (2001).
[19]. **X. Q. Shi, Z. P. Wang, W. Zhou, H. J. L. Pang and Q. J. Yang,** J. Electron. Packaging **124**, 85 – 90 (2002).
[20]. **P. Adeva, G. Caruanan, O. A. Ruano and M. Torralba,** Mater. Sci. Eng. A 194, 17 –23 (1995).
[21]. **F. A. Mohamed, K. L. Murty and J. W**. Morris, Metall. Trans. 4, 935 – 940 (1973).